Publications

Available Online

J. Sci. Res. **1**(3), 409-421 (2009)

JOURNAL OF
SCIENTIFIC RESEARCH
www.banglajol.info/index.php/JSR

Nematic van der Waals Free Energy

A. Oukouiss[1] **and A. Daanoun**[2]

[1]Département de Physique, Faculté Pluridisciplinaire de Nador, B.300, 62700, Selouane, Nador, Morroko

[2]Laboratoire de Physique Applique, Faculté des Sciences et Technique de Tanger, B.P. 416 Tanger, Morroko

Received 22 January 2009, accepted in final revised form 11 July 2009

Abstract

We develop the calculation of free energy in a nematic phase for a model of spherical particles with the long-range anisotropic interaction from the van der Waals theory. We map the gas-liquid equilibrium, which is coupled to a first-order isotropic-nematic transition. We discus how the topology of the phase diagrams changes upon varying the strengths of the isotropic and nematic interactions.

Keywords: Phase diagrams; Nematic interactions; Free energy; Transitions.

DOI: 10.3329/jsr.v1i3.2595 J. Sci. Res. **1**(3), 409-421 (2009)

1. Introduction

In some systems, melting from the solid to the liquid is not a single transition, but occurs as a series of transitions into intermediate states liquid crystal phases. These phases are the states of aggregation that are intermediate between the solid and the liquid. As is well known, liquid crystals exhibit a rich variety of phases [1]. One of the simplest (and better understood) is the nematic phase which is caracterized by positional disorder and long-range orientational order. The relation between the nature of the molecular interaction and the resulting phase diagram is the central theme of equilibrium statistical mechanics [2-4]. For systems with only pair interactions, to which we will restrict ourselves here, a small change in the range of the pair potential can already induce a qualitative change in the topology of the phase diagram [5, 6] This raises, therefore, the general question of how many topologically distinct phase diagrams can be generated from a given family of pair potentials. This question is of practical interest in situations where the pair potential can to some extent be prescribed (e.g., by chemical engineering techniques as is of current use in colloid science [7, 8]). The determination of phase diagram is, however, a very demanding task, and, therefore, the answer to the question raised is not generally available. In the

---

[1] *Corresponding author*: aoukouiss@yahoo.fr

particular case of systems of spherical molecules with simple pair interaction (of the Lennard-Jones type, say) convincing evidence has nevertheless been obtained already that only three topologically distinct types of phase diagrams can be produced by such potential. If the amplitude of the pair potential is used as temperature scale and the range of the repulsions is used to define the density scale, then the family of potentials considered did depend only on one additional parameter, fixing the range of the attractions (relative to the range of the repulsions). The results could then be classified into three categories corresponding to long-ranged, intermediate-ranged, and short-ranged attractions with phase diagrams exhibiting, respectively, a gas-liquid critical point, no critical point, and an (isostructural) solid-solid critical point. The corresponding evidence is partly experimental [9, 10], partly numerical [11,12] and partly theoretical [13,14]. Phase diagrams of systems interacting via density dependent potentials, with a constant excluded volume, can exhibit two phase transitions: gas-liquid and liquid-liquid [15-17]. Systems which exhibit transition to a nematic phase have already been examined by many authors. Onsager [18] did show that particles of a sufficiently anisotropic shape, e.g. long rods or flats discs, form a nematic phase at high densities. Baus *et al.* [19] have used a density-functional theory for the study of the isotropic-nematic transition of hard ellipsoids. They found that the theory predicts a stable nematic phase, both for rodlike and disklike molecules, as a result of competition between the orientational entropy and the anisotropic excluded volume effects. This phase has been confirmed by computer simulations for hard ellipsoids [19, 20] spherocylinders [21-24] and for hard spheres [25]. Recently Mishra *et al.* [26, 27] have used the mean spherical approximation and the percus-Yevick integral equation theories to calculate the free energy functional for the nematic phase. A first-order isotropic-nematic transition is to be found in the liquid regime, although these authors do not present results for the phase diagram. They expressed the two-particle density distribution ρ in terms of order parameters and solved the resulting equation for values of order parameters ranging from zero to some maximum value. They constructed a free energy functional and used it to determine the value of order parameters in the nematic phase by minimizing it.

By computer simulation of a system of ellipsoids Phoung and Shmid [28] showed that in the nematic phase there are two qualitatively different contributions: one that preserves rotational invariance and other that breaks it and vanishes in the isotropic phase. Recently, Lomba and *et al.* [29] have used the Monte Carlo computer simulations to study the phase behaviour of hard sphere Maier-Saupe spins systems. According to this simulation this system undergoes a first-order isotropic-nematic transition continuously coupled to a gas-liquid transition.

In our early extensive study of the phase behaviour of the Heisenberg model [30, 31] we have generalized the van der Waals theory for anisotropic interactions to study the phase behaviour of a system of particles with magnetic exchange interactions.

In the present investigation we perform a similar study. We will use the nematic Maier-Saupe interactions [3-5] and the extended van der Waals theory [30, 31] to calculate the free energy functional for the nematic phase and examine the isotropic-nematic transition. The value order parameter has been found by minimization of the reduced Helmholtz free energy functional in terms of order parameter.

This paper is organized as follows. In sec. 2 we introduce our model for the anisotropic potential. The free energy functional for the nematic phase will be computed in sec. 3 from a van der Waals approximation. The phase diagrams will be presented in sec. 4 while sec. 5 contains our discussions and conclusions.

2. The Molecular Interactions

We consider a system of *N* identical spherical molecules with an embedded anisotropy (such as an electric or magnetic moment). The position and orientation of these molecules will be specified, respectively, by the coordinates (r_i) of their center of mass and the orientations (s_i) of a unit spin variable ($s_i^2 = 1$) placed at this center. The pair potential between two such molecules (say, *i*=1, 2) will be assumed to depend on their relative distance, $|r_1 - r_2|$, and on their relative orientation, $s_1.s_2$. The interaction potential between two such molecules, $V(r_1, r_2, s_1.s_2)$, will be taken to be of the form :

$$V(r_1, r_2; s_1.s_2) = V_{HS}(r_{12}) + V_1(r_{12}) + V_{MS}(r_{12}; s_1.s_2), \tag{1}$$

where the hard-sphere repulsion $V_{HS}(r_{12})$ is given by

$$V_{HS}(r_{12}) = \begin{cases} \infty & \text{if } x_{12} \le 1 \\ 0 & \text{if } x_{12} > 1 \end{cases}, \tag{2}$$

where $x_{12} = r_{12}/\sigma$ is the reduced distance and σ which fixes the range of the repulsion, is the hard-sphere diameter. The second term $V_1(r_{12})$ of Eq. (1) represents the isotropic (spin-independent) interactions and $V_{MS}(r_{12}; s_1.s_2)$ the anisotropic (spin-dependent) interactions. For simplicity, the isotropic interaction will be represented by an inverse-power attraction [30-32]

$$V_1(r_{12}) = \begin{cases} 0 & \text{if } x_{12} < 1 \\ -\varepsilon_1\, \phi_1(x_{12}) & \text{if } x_{12} \ge 1 \end{cases}, \tag{3}$$

where $\phi_1(x_{12}) \ge 0$, with $\phi_{12}(\mathrm{x}_{12}=1)=1$, as appropriate to anisotropic interactions of amplitude $\varepsilon_1 \ge 0$ and

$$\phi_1(x_{12}) = 1/(x_{12})^{n_1}, \tag{4}$$

with n_1 fixing the range of the attractions. As shown [5, 32, 33] elsewhere, with $V_1(r_{12})$ as the potential, the isotropic liquid is thermodynamically stable provided $3 < n_1 < 7.8$. Henceforth we will take $n_1 = 6$, in which case (3)-(4) represents the standard van der Waals (vdW) potential

$$V_{vdW} = V_1(r_{12}). \tag{5}$$

For the anisotropic interactions, we take the Mayer-Saupe nematic interaction

$$V_{MS} = V_2(r_{12}).P_2(s_1.\, s_2) \tag{6}$$

where $P_2(s_1.s_2)=\frac{1}{2}[3(s_1.s_2)^2 \text{-}1]$ is the Legendre polynomial of order 2 and $V_2(r_{12})$ is the radial factor of amplitude ε_2

$$V_2(r_{12})=\begin{cases} 0 & \text{if} \quad x_{12}<1 \\ -\varepsilon_2\ \phi_2(x_{12}) & \text{if} \quad x_{12}\geq 1 \end{cases} \tag{7}$$

will likewise be taken to be of the inverse-power type

$$\phi_2(x_{12})=1/(x_{12})^{n_2}, \tag{8}$$

with a range fixed by n_2. The final pair potential of our Maier-Saupe model can thus be written

$$V(r_1,r_2;s_1.s_2)=V_{HS}(r_{12})+V_1(r_{12})+V_2(r_{12}).P_2(r_{12};s_1.s_2) \quad , \tag{9}$$

with the radial factors fixed by (3)-(4), (7)-(8), or explicitly,

$$V_2(r_{12})=\begin{cases} \infty & \text{if } x_{12}<1 \\ -\varepsilon_1\left\{\dfrac{1}{(x_{12})^{n_1}}+\dfrac{1}{2}[3\,(s_1.s_2)^2\text{-}1]\ \dfrac{\gamma}{(x_{12})^{n_2}}\right\} & \text{if } x_{12}\geq 1 \end{cases} \tag{10}$$

where $x_{12}=r_{12}/\sigma$, while ε_1 fixes the energy scale and $\gamma=\varepsilon_2/\varepsilon_1$ measures the strength of the nematic interactions. The reduced potential V/ε_1 thus depends on three positive parameters $\{\gamma,n_1,n_2\}$.

3. The free energy

For a system of *N* molecules enclosed in a volume *V* at the equilibrium temperature *T*, the phase behaviour can be deduced from the Helmholtz free energy, *F*(*N*,*V*,*T*). In terms of the intensive property, *f* = *F/N*, we have for the (Helmholtz) free energy per particle, $f=f(\rho,T)$, where ρ is the number density, $\rho=N/V$. From $f=f(\rho,T)$ we can obtain the pressure, $p=p(\rho,T)$, and the chemical potential, $\mu=\mu(\rho,T)$, by using the following well known thermodynamic relations [2]:

$$p=\rho^2\frac{\partial f}{\partial\rho}\ ;\ \mu=\frac{\partial}{\partial\rho}(\rho f)\ ; \tag{11}$$

and, knowing *p* and μ we can find the coexisting densities (ρ_1,ρ_2) of phase 1 and phase 2 by solving, for each *T*, the following two-phase equilibrium conditions [2]:

$$p_1(\rho_1,T)=p_2(\rho_2,T)\ , \tag{12}$$

$$\mu_1(\rho_1,T)=\mu_2(\rho_2,T)\,, \tag{13}$$

where P_i, μ_i denote the value of *P*, μ evaluated for phase *i* = (1, 2). Finally, when more than two phases are present for the same *T*, Eqs. (12) and (13) are solved for each pair of coexisting phases, and the thermodynamically stable phase transitions are separated from the thermodynamically metastable phase transitions by constructing the convex envelope to the free energy with the aid of Maxwell's double tangent construction [34]. From the above it will be clear that the construction of a phase diagram for a system described by Eq. (9) is a very labor-intensive task. In order to make this possible we will confine ourselves here to a simple van der Waals approximation for $f(\rho,t)$. We do not, of course, expect this approximation to yield quantitatively correct results.

As is well known, in the vdW-approximation the (hard-sphere) repulsions are described within a free-volume approximation while the attractions are treated within a mean field approximation [5, 33].

The free energy, *F*, of a system with pair-potential of the form defined by Eq. (9) reads

$$F = F_R + \frac{1}{2}\int dr_1 \int ds_1 \int dr_2 \int ds_2 r_2(r_1,r_2;s_1.s_2)\ [V_1(r_{12}) + V_2(r_{12})P_2(s_1.s_2)] \quad , \tag{14}$$

where F_R is the hard-sphere free energy and $\rho_2(r_1,r_2;s_1.s_2)$ denotes the pair-density. Within the mean field approximation the latter is factorized as,

$$\rho_2(r_1,r_2;s_1.s_2) = \rho_1(r_1,s_1)\rho_2(r_2,s_2),$$

where $\rho_1(r,s)$ is the one-particle density. Because Eq. (9) does not couple the position and angular variables we can likewise factorize $\rho_1(r_1,s_1)$ as

$$\rho_1(r,s) = \rho(r)h(s), \tag{15}$$

where $\rho(r)$ is the center of mass density normalized to the average density ρ

$$\frac{1}{V}\int dr\rho(r) = \rho \tag{16}$$

and *h(s)* is the angular distribution of the spin variable normalized to one [30, 31]

$$\int dsh(s) = 1 \tag{17}$$

where, $$\int ds... = \frac{1}{4\pi}\int_0^{2\pi} d\phi \int_0^{\pi} d\theta \sin\theta \tag{18}$$

with θ,ϕ being the polar angles of the unit vector s referred to a laboratory fixed coordinate system. Using Eqs. (15), and (17) the reduced free energy of (14) becomes

$$\begin{aligned} f = \frac{F_{HS}}{N\varepsilon_0} &+ \frac{1}{2N\varepsilon_0}\left[\int dr_1 \int dr_2 \rho(r_1)\rho(r_2)V_1(r_{12})\right]\left[\int ds_1 \int ds_2 h(s_1)h(s_2)\right] \\ &+ \frac{1}{2N\varepsilon_0}\left[\int dr_1 \int dr_2 \rho(r_1)\rho(r_2)V_2(r_{12})\right]\left[\int ds_1 \int ds_2 h(s_1)h(s_2)P_2(s_1.s_2)\right] \end{aligned} \tag{19}$$

where the radial factors can be treated as proposed in [32, 33]. As the angular factor of Eq. (19), we will assume the system to have uniaxial symmetry around the direction $\boldsymbol{n}$, with $n^2 = 1$, of some infinitesimal external (magnetic) field so that

$$h(s) \equiv h(s.n) \equiv h(u), \tag{20}$$

where $s.n = \cos(\theta) \equiv h(u),$ since we can always put $\boldsymbol{n}$ in the direction of the polar **z** axis. The angular average < >, of any axially symmetric function ***g(u)*** of ***u*** then becomes

$$< g > \ = \int ds h(s) g(s) = \int ds h(u) g(u) = \frac{1}{2}\int du\ h(u) g(u), \tag{21}$$

where we used Eqs. (18) and (20).

The hard-sphere free-energy, F_{HS}, can be approximated by (see [5,6,30])

$$F_{HS}(N,V,T) = NK_BT\left[\ln(\rho\Lambda^3)-1\right] + NK_BT.\frac{1}{2}\int_{-1}^{1} du\ h(u)\ln\left[h(u)\right] - NK_BT\ln\alpha(\rho), \tag{22}$$

where the first term is the ideal gas contribution, Λ being the thermal de Broglie wavelength, $\rho = N/V$ the average density. The second represents the orientational entropy and the last term represents the free-volume entropy due to the hard-sphere repulsions of Eq. (2). In particular, we have (see [33])

$$\alpha(\rho) = (1 - \frac{\rho}{\rho_0}) \tag{23}$$

for a fluid phase, with $(\frac{\pi}{6})\rho_{cp}\sigma^3 = 0.495$ being the packing fraction above which the fluid becomes unstable. The second and third terms of Eq.(19), which represents the mean-field exchange energy contribution of the isotropic and nematic interactions defined by Eqs. (3) and (7), becomes (see [30])

$$-\phi_1 - \gamma\phi_2 \int ds_1 \int ds_2 h(s_1) h(s_2) P_2(s_1.s_2) = -\phi_1 - \gamma\phi_2 < P_l >^2 \tag{24}$$

where $\gamma = \varepsilon_2/\varepsilon_1$, $\varepsilon_l(l = 1,2)$ are the amplitudes defined in Eqs. (3) and (7) and ϕ_l denote the radial average defined in Eqs. (3) and (7):

$$\phi_l = \frac{1}{2N}\int dr_1 \int dr_2 \rho(r_1)\phi_l(\frac{r_{12}}{\sigma})\rho(r_2). \tag{25}$$

with $\phi_l(x_{12})$ defined by Eq. (3) and (7).

For a fluid phase, $\rho(r) \equiv \rho,$ Eq. (25) reduces to the cohesion energy

$$\phi_l = 2\pi\rho\sigma^3 \int_1^{\infty} dx x^2 \phi_l(x) \tag{26}$$

which, for the inverse power potentials of sec. 2, becomes

$$\phi_l = \frac{4\pi\rho\sigma^3}{n_l - 3} \tag{27}$$

By using Eqs. (22) and (24), the reduced free energy of Eq. (19) becomes now

$$f = t\left[\ln(\rho\Lambda^3) - 1\right] + \frac{t}{2}\int_{-1}^{1} duh(u)\ln\left[h(u)\right] - t\ln\alpha(\rho) - \phi_1 - \gamma\phi_2 < P_2 >^2 \tag{28}$$

where $t = k_B T/\varepsilon_1$ is the reduced temperature T, and ε_1 is the amplitude of the isotropic attraction appearing in Eq. (3).

In order to find the true equilibrium distribution, $h_0(u)$, we minimize Eq. (28) with respect to $h_0(u)$ under the constraint $\frac{1}{2}\int_{-1}^{1} duh(u) = 1$, i.e.,

$$\frac{\delta}{\delta h(u)}\left[f + \frac{c}{2}\int_{-1}^{1} du' h(u')\right] = 0 \tag{29}$$

where c is a constant. By using Eq. (28), Eq. (29) becomes

$$\frac{t}{2}\ln\left[h(u)\right] + \frac{t}{2} - 2\gamma\phi_2 < P_2 > \frac{P_2(u)}{2} + \frac{c}{2} = 0 \tag{30}$$

The resulting extremum condition can be written

$$t\left[\ln h_0(u) + C\right] = 2\gamma\phi_2 < P_2 >_0 P_2(u) \tag{31}$$

where $C = 1 + \frac{c}{t}$. The solution to Eq.(31) can be written in the standard mean-field form

$$h_0(u) = \frac{\exp(qp_2)}{N(q)} \tag{32}$$

where, $$N(q) = \frac{1}{2}\int_{-1}^{1} du \exp(qP_2(u)) = \sqrt{\frac{2}{3}}\frac{\exp(q)}{\sqrt{q}} D(\sqrt{\frac{3q}{2}}) \tag{33}$$

fixes the normalisation $\left[C = \ln N(q)\right]$; D denotes the Dawson function such that:

$$D(x) = \exp(-x^2)\int_{1}^{x} \exp(t^2)dt \tag{34}$$

and the order parameter q is determined self-consistently by Eq. (31) or, equivalently,

$$q = 2\frac{\gamma}{t}\phi_2 m \tag{35}$$

where $m = < P_2(u) >_0$.

Switching from the order parameter ***q*** to the new order parameter ***m***, we can rewrite the self-consistency condition:

$$m = \frac{1}{2}\int_{-1}^{1} duP_2(u)h_0(u) = \frac{1}{2}\left(\frac{\exp(q)}{qN(q)} - 1 - \frac{1}{q}\right), \tag{36}$$

By using Eqs. (32), (33), (35) and (36) we can rewrite the term $\frac{t}{2}\int_{-1}^{1} du h_0(u)\ln\left[h_0(u)\right]$ in (28) as:

$$2\gamma\phi_2 m^2 - t\ln N(q) \quad , \tag{37}$$

Our total reduced free energy defined in (28) becomes now:

$$f = t\left[\ln(\rho\Lambda^3)-1\right] - t\ln\alpha(\rho) - \phi_1 + \gamma\phi_2 m^2 - t\ln N(q) \tag{38}$$

with $q = 2\frac{\gamma}{t}\phi_2 m$. $N(q)$ and m are determined, respectively, from Eqs. (33) and (36).

In the following we will choose m as a new order parameter instead of q because q is unbounded $(0 \le q \le \infty)$ whereas m is bounded $(0 \le m \le 1)$.

According to the values of m we have then either isotropic phases $(m = 0)$ or nematic phases $(m \ne 0)$.

In order to determine the equation of the borderline which separates the two phases, we will perform a study similar to the one used in [30].

Before doing this let us to give the behaviour of the order parameter $m(q)$ when $q \to 0$: in this case Eq. (33) becomes

$$N(q \to 0) \cong (1 + \frac{q^2}{10} + \frac{8q^3}{15}) \tag{39}$$

Then, Eq. (36) becomes

$$m(q \to 0) \cong \frac{q}{5} - \frac{7q^2}{30}. \tag{40}$$

By using Eq. (35), Eq. (40) can be rewritten as

$$(\frac{2\gamma^*}{5} - 1) = \frac{14}{15}\gamma^{*2} m \tag{41}$$

where $\gamma^* = \frac{\gamma\phi_2}{t}$. Then $\gamma^* \to \frac{5}{2}$ as $q \to 0$.

By plotting the curves, q versus γ^* or γ^* versus q with $\gamma^* = q/2m$ and $m(q)$ given by Eq. (36), we see that this curve can be divided into two branches: N' and N (see Fig. 2a,b). The N' branch is the unphysical branch because q is a decreasing function of γ^*. Furthermore, on this branch the reduced free-energy per unit volume ηf is a concave function of the reduced density $\eta = \pi\rho\sigma^3/6$ (see Fig. 2c). The N branch, however, is the physical branch because, in addition to the fact that q is an increasing function of γ^*, the reduced free-energy per unit volume ηf is a convex function of η (see Fig. 2c).

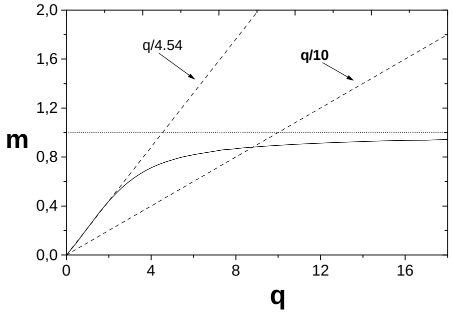

Fig. 1. Graphical representation of the self-consistency Eq. (36), indicating that a nematic phase can exist only for $2\gamma^* > 4.54$.

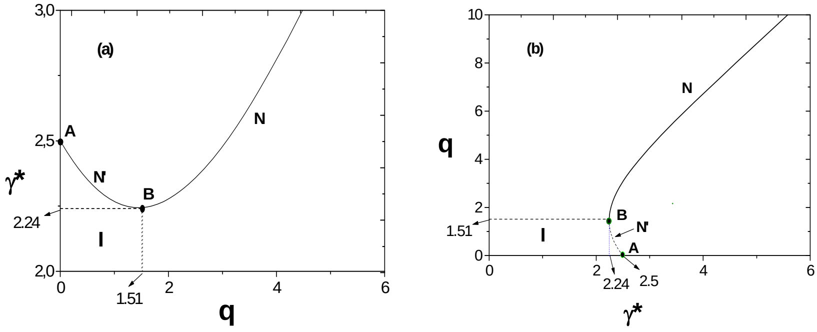

Fig.2. (a, b) Graphical representations of the equation, $\gamma^* = \frac{q}{2m}$.

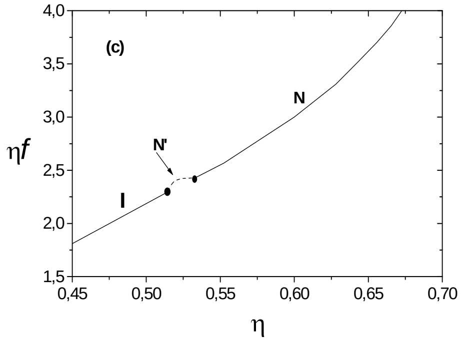

Fig. 2c. Isotropic (I), unphysical nematic (N´) and physical nematic (N) branches of the reduced free energy per unit volume η^f versus the reduced density , for $\Gamma^* = \gamma(n_1\text{-}3)/(n_2\text{-}3) = 1.4$ and $t = 0.7$.

From Fig. 1b we see that the curve is discontinuous, i.e, the parameters q or m are not continuous. The point $(\gamma^* = 1.51,\ q = 2.24)$ is determined by solving the equation

$$\frac{\partial \gamma^*(q)}{\partial q} = 0 \tag{42}$$

with $\gamma^* = \dfrac{q}{2m}$ and m given by Eq. (36).

Therefore, the nematic phase can only occur for q larger than 1.51 or γ^* larger than 2.24. In other words, the isotropic-nematic transition is always of the first-order type because the order parameter q has to jump from q to $q \geq 1.51$.

4. Phase Diagrams

From a system of number density ρ and reduced temperature $t = k_B T/\varepsilon_1$, Eqs. (35), (36) and (38) yield $f = f(\rho, t)$, and from f we obtain the pressure p and chemical potential μ using the well-known thermodynamic relations

$$p = \varepsilon_1 \rho^2 \frac{\partial f}{\partial \rho} \quad , \quad \mu = \varepsilon_1 f + \frac{P}{\rho} \tag{43}$$

We will consider the competition between two types of uniform fluid phases: the isotropic (I) fluid phase (phase 1) without orientational order (m=0), and the nematic (N) fluid phase (phase 2) for which the spin variables are, on average, aligned along some director ($m \neq 0$). We will also use the packing fraction $\eta = \pi\rho\sigma^3/6$ as the reduced density variable. The two-phase equilibrium conditions can then be written

$$P_1(\rho_1, t) = P_2(\rho_2, t), \tag{44}$$

$$\mu_1(\rho_1, t) = \mu_2(\rho_2, t), \tag{45}$$

where the indices 1, 2 refer to phases 1 and 2, respectively. Eqs. (44) and (45) are equivalent to the double tangent construction on the free energies obtained from Eqs. (35), (36) and (38). When more then one transition is possible, the equilibrium transition is found by constructing the convex envelope to the free energies. From Eqs. (38) and (43) the pressure of the fluid phase can be written as

$$\frac{p}{\rho\varepsilon_1} = \frac{t}{\alpha(\rho)} - \phi_1 - \gamma\phi_2 m^2 \tag{46}$$

where $\alpha(\rho)$ is given by (23) and $\phi_l\,(l = 1, 2)$ by (27). The orientational order parameter, $m = m(\rho, t)$, is obtained by solving Eq. (35), yielding $p = p(\rho, t)$ and $\mu = \mu(\rho, t)$. From Eq. (46) we obtain the critical point. The coordinates (t_c, η_c) of the critical point are given by (see [5, 6]):

$$t_c = \frac{32}{3(n_0 - 3)\eta_c} \quad ; \quad \eta_c = \frac{\eta_0}{3} \tag{47}$$

There is no tricritical point because the isotropic-nematic transition is always first-order.

In the isotropic phase m=0, Eq. (46) embodies the standard liquid-gas transition, with terminates in the vdW critical point of (47). Combining this isotropic gas (IG)-isotropic liquid (IL) transition with the isotropic fluid (IF)-nematic fluid (NF) transition, one obtains the phase diagram of the fluid phases in the $\eta - t$ plane.

By using the following reduced thermodynamic variables:

$$\text{and} \quad \begin{matrix} t^* = \dfrac{t}{\phi_1}, \; f^* = \dfrac{f}{\phi_1}, \; p^* = \dfrac{p}{\phi_1}, \\ \Gamma^* = \gamma \dfrac{\phi_2}{\phi_1} = \gamma \dfrac{n_1 - 3}{n_2 - 3}, \quad (\gamma = \dfrac{\varepsilon_2}{\varepsilon_1}) \end{matrix} \quad , \tag{48}$$

we remark that this phase diagram does not depend on the three parameters $\{\gamma, n_1, n_2\}$ separately but only on the combination $\Gamma^*= \gamma(n_1-3)/(n_2-3)$ and not on the various strength (ε_l) and range (n_l) parameters separately. In other words, the phase behaviour is monitored by the relative strengths of the potentials, $\gamma = \varepsilon_2/\varepsilon_1$, and not by the range ($n_l$) of the potentials, i.e., changing (n_l) at constant $\varepsilon_1/(n_1-3)$ has no effect on the phase behaviour.

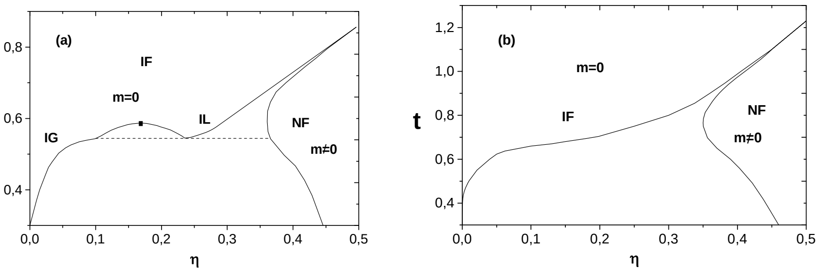

Fig. 3. The two topologically distinct types of phase diagrams in the reduced temperature ($t = k_B T / \varepsilon_0$)-reduced density ($\eta = \pi\rho\sigma^3/6$) plane as obtained from the energy (38); (a) $\Gamma^* = 1$, (b) $\Gamma^* = 1.4$.

5. Results and conclusions

We have studied the phase diagram of a system of particles interacting via both nematic and isotropic interactions by using the extended vdW theory [30, 31]. As is well known, in van der Waals theory the free energy is written as the sum of a free- volume entropy term describing the repulsions and a mean-field energy term describing the attractions [5, 6]. This theory is simple and flexible. It is also fairly realistic since the resulting phase diagrams mimic very closely those obtained from more sophisticated theories and simulations, whenever available [26, 27, 29]. On this basis we have found that the topology of the phase diagrams depends on the value of $\Gamma^{*} = \gamma(n_1\text{-}3)/(n_2\text{-}3)$. According to the value of Γ^{*}, there are two topologically distinct types of phase diagrams (see Fig. 3). For weakly anisotropic fluids, $0<\Gamma^{*}< 1.0863$ all the phase diagrams have IG-IL and IL-NL transition (Fig. 3a). For temperatures below the triple point temperature t_t there is a single first-order transition, namely IG-NL transition. Above t_t there are two first-order transitions, namely a IG –IL transition ending at the critical point (filled square) of (47) and a first-order IL-NL transition. For $t > t_c$ there is only a first-order IF-NF transition. For stronger nematic anisotropies, $\Gamma^{*}>1.0863$ the critical point becomes metastable and the phase diagram contains only a IF-NF transition (see Fig. 3.b). From this we conclude that there is no difficulty in stabilizing the nematic liquid phase over a large domain of the temperature-density plane.

Lastly we would like to emphasize that the theory developed here can be extended to other ordered phases. The free energy described here will allow us to study various phenomena of ordered phases. Our work on freezing of simple liquids into crystalline solids is in progress and the results will be reported in near future [35].

Acknowledgments

We gratefully acknowledge enlightening discussions with Prof. M. Baus (ULB) and Z. El Allali for his help in computation.

References

1. P. G. De Gennes, The physics of liquid crystals (Oxford University Press, Clarendon, 1974).
2. D. L. Goodstein, States of matter (Dover, New York, 1985).
3. D. A. Young, Phase Diagrams of the Elements (University of California Press, Berkely, 1991).
4. J. N. Israelachvili, Intermolecular and Surface Forces, 2nd ed. (Academic Press, London, 1992).
5. T. Coussaert and M. Baus, Phys.Rev. E **52**, 862 (1995). doi:10.1103/PhysRevE.52.862
6. M. Baus, T. Coussaert, and R. Achrayah, Physica A **232**, 575 (1996). doi:10.1016/0378-4371(96)00167-7
7. W. B.Russel, D. A. Saville and W. R. Schowalter, Colloidal Dispersions, 2nd ed. (Cambridge University Press, Cambridge, 1991).
8. W. C. K. Poon and P. N. Pusey, In Observation, Prediction and Simulation of Phase Transition in Complex Fluids, edited by M. Baus et al. (Kluwer, Dordrecht, 1995) p. 3.
9. J. S. Van Duijneveld, A. W. Heinen, and H. N. W. Lekkerkerker, Europhys. Lett. **21**, 369 (1993). doi:10.1209/0295-5075/21/3/019
10. S. M. Ilet, A. Orrock, W. C. K. Poon, and P. N. Pusey, Phys. Rev. E **51**, 1344 (1995). doi:10.1103/PhysRevE.51.1344
11. P. G. Bolhuis, M. H. J. Hagen, and D. Frenkel, Phys. Rev. E **50**, 4880 (1994). doi:10.1103/PhysRevE.50.4880
12. C.N. Likos, T. Nemeth, and H. Lowen, J. Phys.: Condens. Matter **6**, 10965 (1994). doi:10.1088/0953-8984/6/50/007
13. C. F. Tejero, A. Daanoun, H. N. W. Lekkerkerkr, and M. Baus, Phys.Rev. E **51**, 558 (1995). doi:10.1103/PhysRevE.51.558
14. C. Rascon, G. Navascues, and L. Mederos, Phys. Rev. B **51**, 14799 (1995). doi:10.1103/PhysRevB.51.14899

15. G. Monaco, S. Falconi, W. A. Crichton, M. Mezouar, Phys. Rev. Lett. **90**, 255701 (2003). doi:10.1103/PhysRevLett.90.255701
16. S. V.Buldyrev, H. E.Stanley, Physica A **330**, 124 (2003). doi:10.1016/j.physa.2003.08.003
17. A. Daanoun, Eur. Phys. J. B **531**, 61 (2006). doi:10.1140/epjb/e2006-00344-1
18. L. Onsager, Proc. N. Y. Acad. Sci. **51**, 627 (1949).
19. J. L. Colot, X-G Wu, H. Xu, and M. Baus, Phys. Rev. **A** 38, 2022 (1998). doi:10.1103/PhysRevA.38.2022
20. D. Frenkel, Mol. Phys. **60**, 1 (1987). doi:10.1080/00268978700100011
21. D. Frenkel, H. N. W. Lekkerkerker, and A.Stroobants, Nature **332**, 822 (1988). doi:10.1038/332822a0
22. D. Frenkel, J. Phys. Chem. **92**, 3280 (1988). doi:10.1021/j100322a042
23. J. A. C. Veerman and D. Frenkel, Phys. Rev. A **41**, 3237 (1990). doi:10.1103/PhysRevA.41.3237
24. S. C. McGrother, D. C.Williamson, and G. Jackson, J. Chem. Phys. **104**, 6755 (1996). doi:10.1063/1.471343
25. M. J. Blair and G. N. Patey, Phys. Rev. E **57**, 5682 (1997). doi:10.1103/PhysRevE.57.5682
26. P. Mishra and Y. Singh, Phys. Rev. Lett. **97**, 177801 (2006). doi:10.1103/PhysRevLett.97.177801
27. P. Mishra, S. Lata Singh, J. Ram, and Y. Singh, J. Chem. Phys. **127**, 044905 (2007). doi:10.1063/1.2752170
28. N. H. Phoung and F. Schmid, J. Chem. Phys. **119**, 1214 (2003). doi:10.1063/1.1577322
29. E. Lomba, C. Martin, and N. Almarza, Phys. Rev. E **74**, 021503 (2006). doi:10.1103/PhysRevE.74.021503
30. A. Oukouiss and M. Baus, Phys. Rev. E **55**, 7242 (1997). doi:10.1103/PhysRevE.55.7242
31. A. Oukouiss and M. Baus, J. Chem. Phys. **109**, 6157 (1998). doi:10.1063/1.477243
32. M. Baus and R. Achrayah, J. Phys.: Condens. Matter **8**, 9633 (1996). doi:10.1088/0953-8984/8/47/075
33. A. Daanoun, C. F. Tejero, and M. Baus, Phys. Rev. E **50**, 2913 (1994). doi:10.1103/PhysRevE.50.2913
34. R. T. De Hoof, Thermodynamics in Material Science (McGraw-Hill, New York, 1993).
35. A. Oukouiss, A. Daanoun, and M. Baus (in preparation).